Optical transmission and laser structuring of silicon membranes

Saulius Juodkazis[1], Yasufumi Nishi[1], Hiroaki Misawa[1], Vygantas Mizeikis[2], Olivier Schecker[3], Reimar Waitz[3], Paul Leiderer[3], and Elke Scheer[3]

[1] *Research Institute for Electronic Science, Hokkaido University, Sapporo 001-0021, Japan*

[2] *Division of Global Research Leaders, Research Institute for Electronics, Shizuoka University, 3-5-1 Johoku, Naka-ku, Hamamatsu 432-8561, Japan*

[3] *Department of Physics, University of Konstanz, D-78457 Konstanz, Germany*

saulius@es.hokudai.ac.jp;paul.leiderer@uni-konstanz.de;elke.scheer@uni-konstanz.de

Abstract: The optical linear and nonlinear properties of $\sim$ 340-nm-thick Si membranes were investigated. The investigation included both experiments in which the reflection and transmission from the membranes were measured, and finite differences time domain simulations. The linear optical transmission of the Si membranes can be controlled by changing the thickness of a thermally grown oxide on the membrane. Illumination of the membranes with high levels of irradiation leads to optical modifications that are consistent with the formation of amorphous silicon and dielectric breakdown. When irradiated under conditions where dielectric breakdown occurs, the membranes can be ablated in a well-controlled manner. Laser micro-structuring of the membranes by ablation was carried out to make micrometer-sized holes by focused fs-pulses. Ns-pulses were also used to fabricate arrays of holes by proximity-ablation of a closely-packed pattern of colloidal particles.

OCIS codes: (190.5970) Semiconductor nonlinear optics; (350.3850) Materials processing; (230.4685) Optical microelectromechanical devices;

References and links

1. M. M. Roberts, L. J. Klein, D. E. Savage, K. A. Slinker, M. Friesen, G. Celler, M. A. Eriksson, and M. G. Lagally, "Elastically relaxed free-standing strained-silicon nanomembranes," Nature Materials **5**, 388–393 (2006).
2. W. M. Choi, J. Song, D.-Y. Khang, H. Jiang, Y. Y. Huang, and J. A. Rogers, "Biaxially stretchable "wavy" silicon nanomembranes," NanoLetters **7**, 1655–1663 (2007).
3. C. C. Striemer, T. R. Gaborski, J. L. McGrath, and P. M. Fauchet, "Charge- and size-based separation of macromolecules using ultrathin silicon membranes," Nature **445**, 749–753 (2007).
4. B. A. Fairchild, P. Olivero, S. Rubanov, A. D. Greentree, F. Waldermann, R. A. Taylor, I. Walmsley, J. M. Smith, S. Huntington, B. C. Gibson, D. N. Jamieson, and S. Prawer, "Fabrication of Ultrathin Single-Crystal Diamond Membranes," Adv. Mat. **20**, 4793–4798 (2008).
5. S. Tomljenovic-Hanic, A. D. Greentree, C. M. de Sterke, and S. Prawer, "Flexible design of ultrahigh-Q microcavities in diamond-based photonic crystal slabs," Opt. Express **17**, 6465–6475 (2009).
6. D. C. Guhr, D. Rettinger, J. Boneberg, A. Erbe, P. Leiderer, and E. Scheer, "Influence of laser light on electronic transport through atomic-size contacts," Phys. Rev. Lett. **99**, 086801/1–4 (2007).
7. J. D. Thompson, B. M. Zwickl, A. M. Jayich, F. Marquardt, S. M. Girvin, and J. G. E. Harris, "Strong dispersive coupling of a high-finesse cavity to a micromechanical membrane," Nature **452**, 72 – 75 (2008).

#111714 - $15.00 USD Received 21 May 2009; revised 10 Jul 2009; accepted 13 Aug 2009; published 14 Aug 2009

8. N. Kang, A. Erbe, and E. Scheer, "Electrical characterization of DNA in mechanically controlled break-junctions," New J. Phys. **10**, 023030/1–9 (2008).
9. R. Waitz, O. Schecker, and E. Scheer, "Nanofabricated adjustable multicontact devices on membranes," Rev. Sci. Instrum. **79**, 093901/1 –5 (2008).
10. J. El-Ali, P. K. Sorger, and K. F. Jensen, "Cells on chips", Nature **442**, 403 – 411 (2006).
11. J. Butschke, A. Ehrmann, E. Haugeneder, M. Irmscher, R. Käsmaier, K. Kragler, F. Letzkus, H. Löschner, J. Mathuni, I. W. Rangelow, C. Reuter, F. Shi, and R. Springer, "PN and SOI wafer flow process for stencil mask fabrication," Proc. SPIE **3665**, 20 – 29 (1999).
12. O. Schecker, "Nano-contacts for ElectroMagnetic NanoSystems (NEMS)," Ph.D. thesis, Institute of Microelectronics, Electromagnetics, and Photonics, Grenoble, France and University of Konstanz, Konstanz, Germany (2008).
13. O. Toader, T. Y. M. Chan, and S. John, "Diamond photonic band gap synthesis by umbrella holographic lithography," Appl. Phys. Lett. **89**, 101117/1–3 (2006).
14. B. Deal and A. S. Grove, "General Relationship for the Thermal Oxidation of Silicon," J. Appl. Phys. **36**, 3770 – 3778 (1965); online calculator at http://ee.byu.edu/cleanroom/OxideThickCalc.phtml.
15. S. A. Vitale and B. A. Smith, "Reduction of silicon recess caused by plasma oxidation during high-density plasma polysilicon gate etching," J. Vac. Sci. Technol. B **21**, 2205–2211 (2003).
16. Y.Yokota, K. Ueno, V. Mizeikis, S. Juodkazis, K. Sasaki, and H. Misawa, "Optical characterization of plasmonic metallic nanostructures fabricated by high-resolution lithography," J. Nanophotonics **1**, 594 (2008).
17. K. Ueno, S. Juodkazis, T. Shibuya, Y. Yokota, V. Mizeikis, K. Sasaki, and H. Misawa, "Nanoparticle plasmon-assisted two-photon photolymerization induced by incoherent excitation source," J. Am. Chem. Soc. **130**, 6928–6929 (2008).
18. H. Morikami, H. Yoneda, K.-I. Ueda, and R. M. More, "Detection of hydrodynamic expansion in ultrashort pulse laser ellipsometric pump-probe experiments," Phys. Rev. E **70**, 035401R/1–3 (2004).
19. E. E. Gamaly, S. Juodkazis, K. Nishimura, H. Misawa, B. Luther-Davies, L. Hallo, P. Nicolai, and V. Tikhonchuk, "Laser-matter interaction in a bulk of a transparent solid: confined micro-explosion and void formation," Phys. Rev. B **73**, 214101 (2006).
20. Y. Izawa, Y. Izawa, Y. Setsuhara, M. Hashida, M. Fujita, R. Sasaki, H. Nagai, and M. Yoshida, "Ultrathin amorphous Si layer formation by femtosecond laser pulse irradiation," Appl. Phys. Lett. **90**, 044107/1–2 (2007).
21. M. J. Birnbaum, "Semiconductor surface damage produced by ruby lasers," J. Appl. Phys. **36**, 3688 – 3689 (1965).
22. D. Bäuerle, *Laser processing and chemistry* (Springer, Berlin, 2000).
23. H.-J. Münzer, M. Mosbacher, M. Bertsch, J. Zimmermann, P. Leiderer, and J. Boneberg, "Local field enhancement effects for nanostructuring of surfaces," J. Microscopy **202**, 129–135 (2001).
24. H. Iwase, S. Kokubo, S. Juodkazis, and H. Misawa, "Suppression of ripples on Ni surface via a polarization grating," Opt. Express **17**, 4388–4396 (2009).
25. K. Yamasaki, S. Juodkazis, S. Matsuo, and H. Misawa, "Three-dimensional microchannels in polymers: one step fabrication," Appl. Phys. A **77**, 371–373 (2003).
26. E. Vanagas, I. Kudryashov, D. Tuzhilin, S. Juodkazis, S. Matsuo, and H. Misawa, "Surface nanostructuring of borosilicate glass by femtosecond nJ energy pulses," Appl. Phys. Lett. **82**, 2901–2903 (2003).
27. F. Hudert, A. Bruchhausen, D. Issenmann, O. Schecker, R. Waitz, A. Erbe, E. Scheer, T. Dekorsy, A. Mlayah, and J.-R. Huntzinger, "Confined longitudinal acoustic phonon modes in free-standing Si membranes coherently excited by femtosecond laser pulses," Phys. Rev. B **79**, 201307R/1 – 4 (2009).

1. Introduction

Nano-structures and nano-devices have at least one cross section smaller or comparable with 100 nm. There is an increasing demand for nano-materials which could be incorporated and integrated into hierarchically larger structures of a sub-millimeter scale. These structures could be used for new applications in the fields of electronics [1, 2], micro-electro-mechanical systems (MEMS) and their optical counterparts (MOEMS).

A particular type of nano-materials are membranes, which have thicknesses of ~ 100 nm and lateral dimensions that can be up to 10^4 times larger than their thickness. They serve as molecular sieves [3] and for slab photonic crystals [4, 5]. Recently, such membranes have been used as meshes for X-ray and electron diffraction experiments, for nano-contact and break-junction fabrication, for the investigation of single electron transport [6], and for opto-mechanical coupling between electromagnetic radiation in an optical cavity [7] where a membrane is potentially applicable for cooling mechanical degrees of freedom. Membranes have also been used

#111714 - $15.00 USD Received 21 May 2009; revised 10 Jul 2009; accepted 13 Aug 2009; published 14 Aug 2009

for very precise control of separation, $\sim$ 10 pm, between atomically sharp nano-contacts, where the nano-gap is controlled mechanically via an actuation of the membrane by a piezo-ceramic stylus [9]. Membrane-based break-junctions should be able to operate in a liquid environment. This makes them attractive for MOEMS and microfluidic applications [10].

Membranes can be made out of silicon-on-isolator (SOI) substrates by a simple wet etching procedure [11, 12]. SOI membranes can also be processed to form arbitrary shapes using deep reactive ion etching [12]. Another advantage of thin freestanding Si membranes is that Si is a standard substrate and therefore it is available almost defect and stress-free, with any desired crystalline orientation, and with various dopants.

A current trend in miniaturization is to incorporate silicon nano-/micro-elements such as membranes, waveguides, gratings, and three-dimensional (3D) structures into opto-mechanical/fluidic/electronic devices. Laser post-processing of micro-chips and optical elements is used to remove, repair, or add new functionality by controlled annealing, ablation, welding/joining and crystallization. These tasks require high laser irradiance. Some optical micro-devices such as 3D lithography masks for polymerization of 3D photonic crystal structures [13] are also subjected to high irradiance, which has been found to affect their performance and compromise their reliability. Hence, the optical, thermal, and mechanical properties of the Si membranes and gratings, their oxidation and degradation need to be investigated to improve applications where high-irradiance or/and ultra-short laser pulses are used.

Here, we report on the optical characterization of $\sim$ 340-nm-thick Si membranes that are optically transparent. The membranes were tested under conditions that ranged from linear transmission through to conditions where amorphisation and ablation occurred. Micrometer-sized holes were laser fabricated through the membranes by focused pulses as well as by proximity ablation using colloidal microspheres. The membranes can be made optically transparent down to 500 nm wavelength. Therefore they could potentially be used for optical imaging of micro-bio objects in micro-fluidic chips.

2. Methods and Materials

Samples were fabricated from SOI wafers consisting of 340 ± 5 nm of Si, 400 ± 15 nm of SiO_2, on a 520 μm substrate of Si (SOITEC, Grenoble) into which we define freestanding single-crystalline membranes of Si (see Fig. 1(a)). We use a two step wet etching process on the backside of the wafer by KOH and HF solutions to remove the Si and SiO_2, respectively [11]. The typical lateral dimensions of the membranes were 0.6×0.6 mm^2 and the thickness was 340 nm with only a few nanometers of native oxide on the membranes. Thermal oxidation at a high temperature ($\sim 1000^{\circ}$C) in air [14] was used to grow layers of oxide on the membranes, thereby reducing the Si thickness and modifying their spectral transmission properties. Figure 1(a) shows the geometry of the used samples and an actual optical image of an oxidized membrane. The growth rate of the oxide layers was governed by oxygen diffusion and followed the established linear-parabolic relation with time according to the Deal-Grove model [14, 15]. As such, the growth rate was weakly dependent on the crystalline orientation. The thickness of oxide could be controlled with a precision of $\sim$ 10 nm. The actual thicknesses of membrane was measured by imaging ellipsometry.

Standard UV-IR (UV 3100PC Shimadzu) and FT-IR (FT/IR-6000TM-M, Jasco) spectrometers were used to measure the transmission and reflection spectra at normal incidence in the visible and the IR regions, respectively. Simulations of the optical properties were carried out using FDTD Solutions (Lumerical, Canada), which is a finite differences time domain (FDTD) software package. Here, we used FDTD to simulate the propagation of plane waves and focused Gaussian beams through the Si membranes at normal incidence. The optical properties of Si and silica were obtained from the database built in to the software package. The simulations

#111714 - $15.00 USD Received 21 May 2009; revised 10 Jul 2009; accepted 13 Aug 2009; published 14 Aug 2009

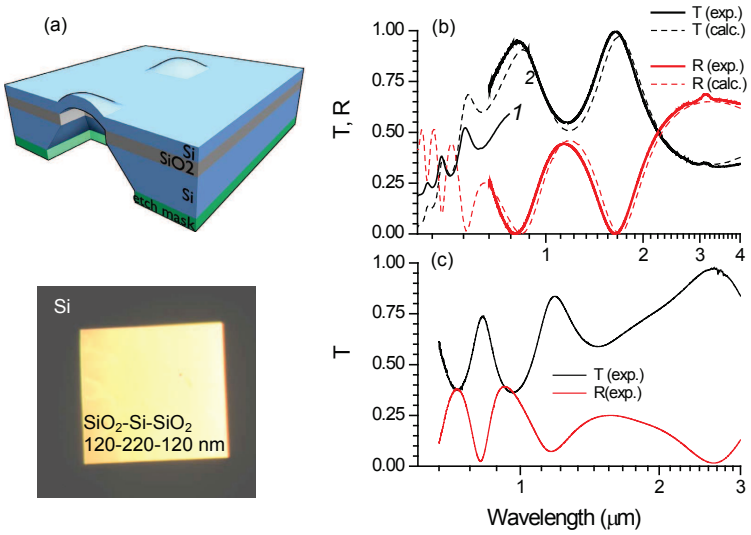

Fig. 1. (a) Schematics of sample (not to scale) and an optical image of a 0.6×0.6 mm^2 oxidized Si-membrane. The linear transmission, T, and reflection, R, spectra of the oxidized (b) and as made silicon membranes (b); thicknesses were SiO_2/Si/SiO_2 of 120/220/120 nm (a) and Si of 340 nm (c), respectively. The spectra *(1)* and *(2)* were measured on different membranes. The FDTD calculations were carried out in a plane wave geometry. The experimental FT-IR reflection spectra were normalized to the reflection from gold; the transmission was normalized to that of air. Spectra were measured for an area of 20×20 μm^2. Note, the scales on the x-axes of the graphs are logarithmic in order to better resolve transmission oscillations.

mirrored focusing conditions that were tested experimentally.

The experiments to test optical transmission and structural modifications were carried out using a femtosecond laser (Hurricane, Spectra Physics), which delivers 150 fs pulses centered around the wavelength of $\lambda_0 = 800$ nm. For transmission measurements, the laser beam of approximately $d = 7$ mm in diameter was focussed by a $f = 250$ mm focal length lens onto the sample. The diameter of the focal spot can be estimated for the Gaussian beam as $2w_0 = \frac{4\lambda}{\pi}\frac{f}{d} \simeq 36$ μm with the axial length of the focal spot equal to twice the Rayleigh length, $2z_R = \frac{8\lambda}{\pi}\left(\frac{f}{d}\right)^2 \simeq 2.6$ mm. Hence, the entire thickness of the membrane was placed in the same region of irradiance. The peak irradiance was calculated assuming a Gaussian intensity distribution $I = E_p/(\sqrt{\pi}t_p\pi w_0^2)$, where E_p and t_p are the energy and duration of laser pulse respectively. This setup was used to measure linear and nonlinear transmission of membranes. The incidence angle of a p-polarized beam was set at 1.5° out of the normal in order to separate the reflected and incident beams and had a minor effect on the measured reflection and transmission.

The power dependencies of the transmitted and reflected energy of femtosecond laser pulses from Si-membrane samples were measured in single-pulse and multi-pulse irradiation modes in order to observe their departure from linear behavior. The transmission and reflection were measured simultaneously for the same laser pulse. In the case of multi-pulse exposure, the same spot of approximately 20 μm in diameter was irradiated by single pulses with increasing energy. For single pulses, the irradiation area was refreshed from shot to shot with simultaneous measurements of transmission and reflection performed with identical photodiodes. Since the measurements were carried out on different membranes the experimental dependencies

#111714 - $15.00 USD Received 21 May 2009; revised 10 Jul 2009; accepted 13 Aug 2009; published 14 Aug 2009

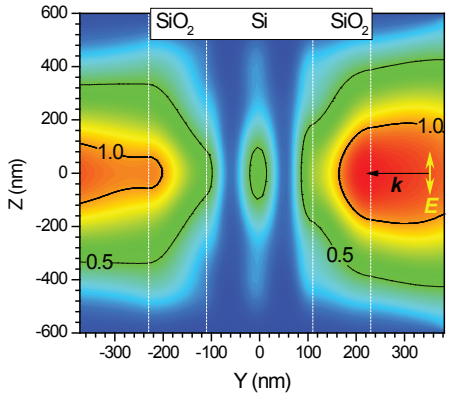

Fig. 2. The light intensity distribution across a SiO_2/Si/SiO_2 (120/220/120 nm; marked by dashed lines) membrane simulated by 3D-FDTD algorithm for a Gaussian beam focused by an objective lens of numerical aperture $NA = 0.5$ (the same NA as in actual FT-IR measurements shown in Fig. 1). The wavelength is approximately 800 nm (374.57 THz). The arrow marks the direction of polarization of the light source $\mathbf{E}(0,0,1)$; The propagation direction was along the wavevector $\mathbf{k}$. The contour lines at intensity levels $I = 0.5;1$ are highlighted.

were normalized to the values obtained at the lowest irradiance where single and multi-pulse measurements yielded the same values.

Ablation of the membranes was carried out by two different approaches: by fs-pulses tightly focused with an objective lens of numerical aperture $NA = 0.9$ and by near-field proximity ablation using colloidal silica microspheres irradiated by 10 ns pulses of Nd:YAG laser at 532 nm wavelength. Structural inspection of the irradiated regions was carried out by optical imaging and by scanning electron microscopy (SEM). Changes in the contrast of the optical images provided evidence for structural changes in the silica, such as the formation of ripples. The existence and nature of the changes was confirmed by SEM inspection.

3. Results and discussion

3.1. Linear optical properties

Thin silicon membranes are transparent even at wavelengths considerably shorter than the fundamental short wavelength of the absorption edge in bulk Si. This absorption edge is defined by the bandgap, $E_g = 1.11$ eV at 300 K, i.e., $\lambda_g[\mu\text{m}] = 1.23975\ [\mu\text{m}]/E_g\ [\text{eV}] \simeq 1.12\ \mu\text{m}$. Hence a thin few-hundreds-of-nanometers silicon film of a high refractive index $n_{Si} \simeq 3.4$ Si strongly modulates the transmission, reflection, and absorption spectra due to interference. In addition, thermal oxidation of the membranes allows tuning the thickness of silicon via formation of an oxide layer [14, 15]. Therefore, thermal oxidation can be used for enhancing or decreasing transmission at the particular wavelength of interest.

Figure 1 shows experimental and FDTD simulations of the transmission spectra of an oxidised membrane and an as made Si membrane. The results from the simulations did not differ by more than 5% in terms of the spectral position and intensity of the interference peaks for the plane wave and Gaussian beam. Since the three dimensional (3D) simulations for a Gaussian pulse were lengthy we show here results obtained for the plane wave. The oxidized membrane (a) was highly transmissive at around the wavelength of 800 nm, which was later used for measurements of the nonlinear transmission and structural modification discussed in Sec. 3.2.

#111714 - $15.00 USD Received 21 May 2009; revised 10 Jul 2009; accepted 13 Aug 2009; published 14 Aug 2009

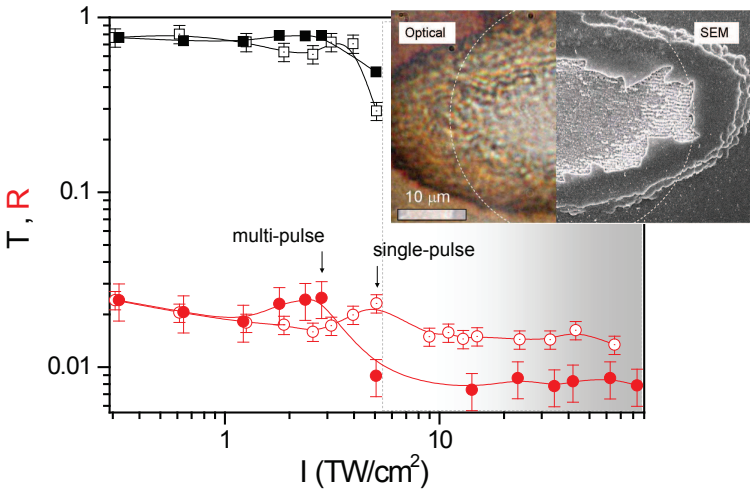

Fig. 3. The transmission, T, and reflection, R, of a SiO_2/Si/SiO_2 (120/220/120 nm) membrane in single and multi-pulse exposure regimes. The lines are drawn as eye guides; the shadowed regions mark the irradiance range where strong structural modifications occurred. The multi-pulse data at the smallest irradiance have been normalized to the values measured in the case on single-pulse irradiation. The inset shows a combined optical and SEM image of the multiply irradiated region on a membrane above damage threshold.

The SiO_2 layers on the membrane act as an anti-reflection coating. The thickness of the layers can be controlled by the duration and temperature of the thermal oxidation, thereby enabling control of the spectral transmission through the membrane.

The small differences between the simulations and the experiment are probably caused by slight deviations in the thickness of the membranes used in the experiments from the membrane thicknesses used in the simulations. Hence the differences between the experimentally measured spectra, and the spectra predicted by the simulations do not affect the general observation that the features in the experimental spectra are completely accounted for by the optical properties and thicknesses of the Si-membrane and thermal oxide.

Figure 2 shows a simulation of the intensity profile when a Gaussian beam at a wavelength of around 800 nm wavelength is focused onto the membrane for which the transmission spectrum is shown in (Fig. 1(b)). The light intensity inside the Si-membrane is equal to only about half of the intensity of the incident light. This is because of the interference caused by the oxide layers on the membrane that act as antireflection coatings.

It is worth noting that the spectral regions where the light is not localized inside the silicon but on the surface of silica (Fig. 2) can be used for plasmonic applications when nano-particles of gold, silver, or copper are formed or deposited on such surfaces. Nano-particles can enhance the field by several orders of magnitude at specific locations (corners and gaps) [16, 17].

3.2. Nonlinear optical properties

In the case of multi-pulse exposure, the very same location of membrane was irradiated in a cumulative mode. The strongest changes were observed in reflection, which increased when the irradiance approached levels at which strong structural modifications began to occur. This happened within $1.5-2.5$ TW/cm^2 irradiance ($\sim 0.22-0.37$ J/cm^2 fluence; see, Fig. 3). When the membranes were exposed to single-pulses (each measurement was carried out on a new spot) such changes occurred at an irradiance which was approximately twice as large. In both

#111714 - $15.00 USD Received 21 May 2009; revised 10 Jul 2009; accepted 13 Aug 2009; published 14 Aug 2009

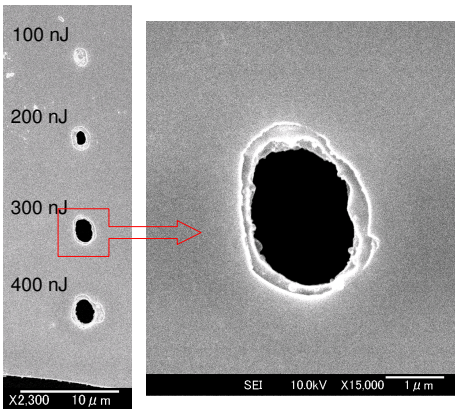

Fig. 4. SEM images of holes ablated in a Si membrane by 20 pulses. Focusing was carried out by an objective lens of $NA = 0.9$.

cases, the reflection gradually increased before it suddenly decreased at large levels of irradiance (Fig. 3). The maximum of reflectivity corresponded to structural changes recognized optically and by SEM observation. An increase in reflectivity is expected at the pre-breakdown irradiance before ablation and hydrodynamic motion of the surface occur. This is because during these processes, the real part of the dielectric function grows faster than the imaginary part [18].

In the case of multi-pulse irradiance an accumulation effect was observed, i.e., the change of transmission and reflection depended of the irradiation dose carried out by previous pulses. It is known that the defects and amorphization of Si created by the preceding pulses at a pre-breakdown threshold irradiance enhance the generation of free electrons and avalanche ionization [19]. Formation of amorphous silicon (a-Si) was reported for Si irradiated by fs-pulses: 0.18 J/cm^2 at 800 nm [20]. The thickness of a-Si was approximately 42 nm after six laser pulses with no changes in the a $\sim$ 2 nm thickness of native oxide observed [20]. The increase of reflectivity in multi-pulse exposure case (Fig. 3) is consistent with formation of amorphous Si at the $\sim$ 0.22 J/cm^2 fluence comparable to the reported 0.18 J/cm^2 value [20].

Note that the changes in the refractive index and absorption modulation due to the thermal effects should occur on a much longer time scale (0.1-1 ns) than the pulse duration and therefore the pulses should not influence the transmission and reflection in single-shot experiments. However, the fs-pulses have a ns-pedestal with intensity smaller by a factor of $\sim$ 200 but total energies of the fs and ns pulses are comparable; this is an important feature for the reflection and transmission measurements. The reflectivity increase in the case of single pulse irradiation (Fig. 3) is attributable to the absorption of the ns-pedestal's trailing part on the defects which already had been formed during tens-of-ns after the fs-pulse irradiance.

At irradiance levels higher than those at which dielectric breakdown occurs, the reflection and transmission are determined by scattering and ablation (shadowed regions in Fig. 3) as revealed by a post-exposure SEM observation. The dielectric breakdown corresponds to plasma formation and the onset of ablation and its effect was more pronounced in the case of multi-pulse irradiation. At pulse irradiances of 40-50 TW/cm^2 the membranes were damaged by cracks (inset of Fig. 3). The possibility of using high laser irradiance for structural modification of the membranes by ablation is discussed next.

#111714 - $15.00 USD Received 21 May 2009; revised 10 Jul 2009; accepted 13 Aug 2009; published 14 Aug 2009

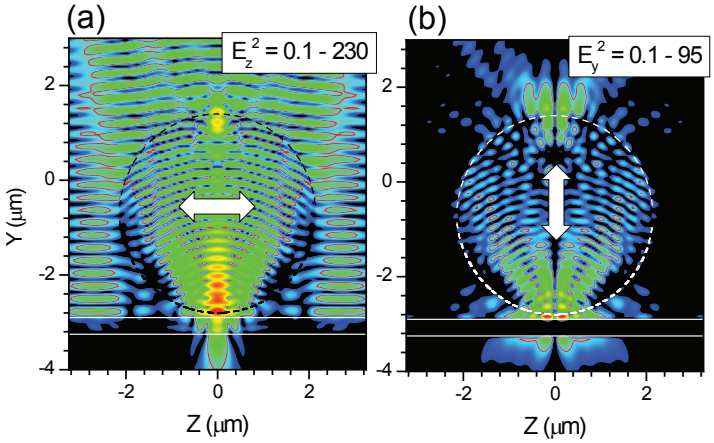

Fig. 5. The near-field intensity distribution of a plane wave $\mathbf{E}(0,0,1)$ propagating through a $4.3-\mu$m silica sphere on a 350 nm Si-membrane for E_z^2 (a) and E_y^2 (b) components; simulations were carried out by a 3D-FDTD algorithm and intensity is plotted on a log-scale. The wavelength of the plane wave was 532 nm. The outline of the sphere and the Si-membrane are marked; the contour lines at intensity level $E_{z,y}^2 = 1$ are also highlighted.

3.3. Structural modifications by focused fs-pulses

The membranes appeared optically more transparent after irradiation by an increasing number of fs-laser pulses (see inset of Fig. 3). It was confirmed by SEM observation that this was the result of partial ablation of silicon, ripples formation [21, 22], and thermal oxidation (Fig. 3). The period of the ripples was approximately $\Lambda = \lambda_0/n_{ox} \simeq 560$ nm, where $n_{ox} \simeq 1.43$ is the refractive index of a silica layer. Ripples can have an aspect ratio close to one [22]; hence the entire thickness of the silicon membrane could be affected by ripples. The increased transmission after multi-pulse irradiation could result from the formation of ripples which have a height comparable to the membrane and oxide layer thickness.

The ripple formation by fs-laser pulses appears as a gradual modification which the membranes apparently withstand. One might wonder whether fs pulses can also be used for drilling small holes into the membranes without fracturing them. Fig. 4 demonstrates that this is indeed possible. Micrometer-sized holes can be ablated through the membranes by exposing them to several femtosecond pulses (Fig. 4). The rims of the holes are less rugged after 10-20 pulse irradiation and they have the same average size as those made by 5-10 pulses. Slight elongation of the holes in the vertical (along the polarization) direction, as seen in Fig. 4, is caused by the ellipticity of the pulse as was revealed by knife-edge measurements of the intensity profile.

3.4. Structural modifications by a proximity ablation using colloidal particles

An alternative technique for ablating micrometer-sized holes in Si substrates relies on irradiating spherical colloidal particles with short laser pulses and making use of the optical near-field enhancement by the spheres [23]. We tried this method on the Si membranes and found that it worked with both fs and ns laser pulses. As test samples we used monolayers of colloidal 4.3 μm-diameter silica microspheres dispersed over the membrane surface and irradiated by nanosecond laser pulses at a wavelength of 532 nm. The expected field enhancement at the sphere-membrane contact point was calculated by 3D-FDTD and is shown in Fig. 5. The enhancement of intensity for the incident polarization, $E_z = 1$, was approximately 200 times. The vertical (to the membrane) E-field, which was absent in the incident light was approxi-

#111714 - $15.00 USD Received 21 May 2009; revised 10 Jul 2009; accepted 13 Aug 2009; published 14 Aug 2009

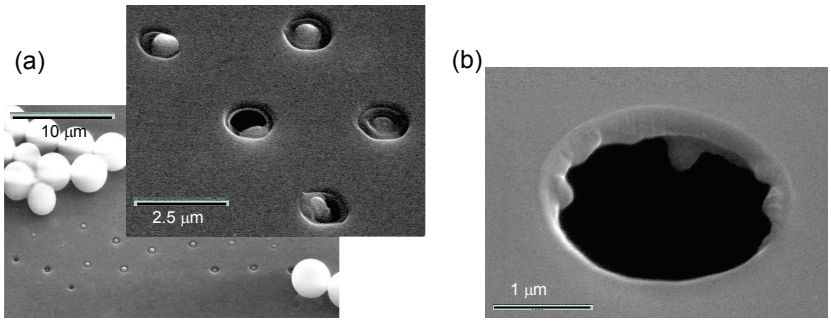

Fig. 6. (a) SEM images of the ablation patterns on a 340-nm-thick Si-membrane. Ablation was carried out by 532nm/10 ns pulses of different pulse energies using $4.3-\mu$m silica spheres dispersed over membrane. (b) Through-hole punched in the membrane.

mately $E_y \simeq 10^2$ just at the microsphere-membrane interface due to the light focusing by a micro-sphere. The vertical to the surface E-field component is efficient in ablation and material removal, also, it does not excite surface electromagnetic wave and can be used for fine structuring of surfaces [24].

Membrane structures obtained by irradiating such samples are shown in Fig. 6. In this case a single ns laser pulse at a wavelength of 532 nm was used as a light source. In the region of the sample where the laser intensity was barely above the ablation threshold, pits formed at the sphere-membrane contact, with some depth distribution due to the poly-dispersity of the microspheres which gives rise to some scatter in the near-field intensity (Fig. 6(a)). However, well above the threshold, well-defined holes through the membrane were generated (Fig. 6(b)).

4. Conclusions

We optically characterized silicon membranes prepared by wet etching and subsequent controlled thermal oxidation. Such membranes can be made transparent in the visible and IR spectral regions. Fabrication of through holes of 1-3 μm in diameter in membrane is possible by tightly focused fs-laser pulses or by proximity ablation using colloidal microspheres.

The abrupt optical transmission and reflection changes caused by multi and single pulse irradiation (after a 0.22 - 0.37 J/cm^2 ramp for multi pulses and about double that for single pulses) correspond to the dielectric breakdown of silicon. The dielectric breakdown threshold measured for membranes was approximately 1.22 times larger than the known threshold for amorphous silicon formation, which occurs at 0.18 J/cm^2 in the case of multi-pulse irradiation.

Ablation of through-holes by uniform illumination of a large area of microspheres can be used to structure the membranes at an irradiance much lower than the threshold of ablation for the bare membrane. In our current experiments, the smallest ablated through-hole was approximately 1 μm in diameter for the 340-nm-thick membrane studied here. However, it should be possible to generate even smaller holes in thinner membranes.

Since the membranes are optically transparent, they could be used in laser tweezing and micro-fluidic applications [10]. The optical transmission of the membranes can be spectrally modified by changing the corresponding thickness of silicon and the oxide as well as by thermally induced expansion. Surface and bulk modifications of materials by femtosecond laser pulse can be used to make holes, bumps of molten surface, or micro-channels [25, 26] for integrated MOEMS applications. The membranes can withstand reversible strains even large than 1%; e.g., deflections of more than 40 μm for a 600 μm-wide membrane were observed [9] leading to an estimation for the maximum elastic strain of about 5% and a maximum force of

#111714 - $15.00 USD Received 21 May 2009; revised 10 Jul 2009; accepted 13 Aug 2009; published 14 Aug 2009

250 mN when the membrane breaks.

The unique combination of mechanical and optical properties of membranes, e.g. their combination of both high-Q factors [7, 27] and high levels of mechanical flexibility are expected to expand functionalities of opto-mechanical/fluidic micro chips.

We thank Pascal Frank and Wilko Westhäuser for assistance with the experiments and Johannes Boneberg for fruitful discussions. Financial support by the Deutsche Forschungsgemeinschaft (SFB 513 and SFB 767), the Center for Applied Photonics in Konstanz, and by Grant-in-Aid No. 19360322 from the Ministry of Education, Science, Sports, and Culture of Japan are gratefully acknowledged.

#111714 - $15.00 USD Received 21 May 2009; revised 10 Jul 2009; accepted 13 Aug 2009; published 14 Aug 2009